Downloaded from rsta.royalsocietypublishing.org

PHILOSOPHICAL TRANSACTIONS OF THE ROYAL SOCIETY A
MATHEMATICAL, PHYSICAL & ENGINEERING SCIENCES

Electron Energy-Loss Spectroscopy for Elemental Analysis [and Discussion]

R. F. Egerton and A. F. Fell

Phil. Trans. R. Soc. Lond. A 1982 **305**, 521-533
doi: 10.1098/rsta.1982.0049

Email alerting service Receive free email alerts when new articles cite this article - sign up in the box at the top right-hand corner of the article or click **here**

To subscribe to *Phil. Trans. R. Soc. Lond. A* go to: **http://rsta.royalsocietypublishing.org/subscriptions**

This journal is © 1982 The Royal Society

Downloaded from rsta.royalsocietypublishing.org

Phil. Trans. R. Soc. Lond. A **305**, 521–533 (1982)
Printed in Great Britain

Electron energy-loss spectroscopy for elemental analysis

By R. F. Egerton
Department of Physics, University of Alberta,
Edmonton, Canada T6G 2J1

Electron-beam microanalysis is most commonly carried out by recording the spectrum of X-rays emitted from a sample. However, an alternative method is to analyse the energy spectrum of electrons transmitted through a thin specimen. For the detection and measurement of elements of low atomic number, this energy-loss method is capable of high sensitivity; detection of less than 10^{-20} g has been reported, while the attainable spatial resolution is probably below 1 nm. After outlining the basic physics involved, the paper gives examples of energy-loss analysis of thin films, intercalation compounds, ceramics and biological samples, and its application to the measurement of radiation damage in organic materials.

1. Introduction

Beams of electrons are relatively easy to produce, for example by thermal emission *in vacuo* from a heated filament and subsequent acceleration by an electric field. For accelerating potentials in the range 10 keV to 1 MeV, the electron wavelength is of less that atomic dimensions and the electrons can be focused with high spatial resolution by electrostatic or magnetic lenses. In consequence, a transmission electron microscope can routinely produce images with a resolution better than 1 nm from many types of specimen.

However, such images provide mainly *structural* information; that is, they are not chemically specific, beyond the fact that regions of high atomic number scatter the electrons more strongly and thus tend to appear darker on the viewing screen. Therefore, attachments are frequently added to the basic instrument to collect additional signals that make possible *analytical* electron microscopy, i.e. the measurement of chemical information on a very fine scale. One way of achieving this is to add an X-ray spectrometer, which measures the wavelength distribution of X-rays created at the specimen by the electron beam (Jefferson, this symposium). Another technique involves incorporating an electron spectrometer to measure the energy spectrum of low-energy Auger electrons that emerge from the sample. In either case, the signal is chemically specific because the photon or electron energies are directly related to the binding energies of inner atomic shells, which in turn are strongly characteristic of each element present.

A third procedure for analytical electron microscopy, which was proposed many years ago (Hillier & Baker 1944) but has only recently achieved popularity, is to place an electron spectrometer in the path of the beam of high-energy *transmitted* electrons to measure the (fractionally) small variations in kinetic energy arising from the various inelastic interactions that have taken place in the specimen (some of which will have resulted in the production of X-rays and Auger electrons). The resulting plot of electron intensity as a function of energy loss (= incident energy minus the measured kinetic energy) is called the electron energy-loss spectrum and the technique itself electron energy-loss spectroscopy (Eels). The aim of this

PHILOSOPHICAL TRANSACTIONS OF THE ROYAL SOCIETY A MATHEMATICAL, PHYSICAL & ENGINEERING SCIENCES

The Royal Society is collaborating with JSTOR to digitize, preserve, and extend access to
Philosophical Transactions of the Royal Society of London. Series A, Mathematical and Physical Sciences.
www.jstor.org

Downloaded from rsta.royalsocietypublishing.org

paper will be to discuss the basic principles of Eels, its advantages and disadvantages compared with other electron-beam methods of microanalysis, and to illustrate some of its capabilities by means of examples.

2. Scattering of an electron beam within a solid

(a) *Elastic scattering*

When an accelerated electron enters a specimen, it may be deflected by the internal electrostatic field of an atom (i.e. by the nuclear field, modified by the screening effect of the surrounding atomic electrons). Because the mass of a nucleus is much greater than that of the incident electron, the latter loses (in most cases) a negligible amount of energy; this type of interaction is therefore known as *elastic* scattering, and is represented in the electron energy-loss spectrum by a sharp peak at zero energy loss (see figure 1).

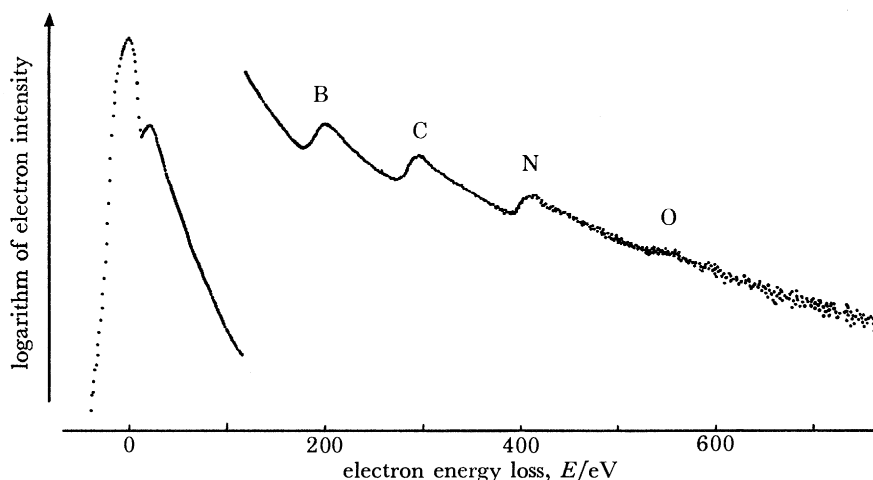

Figure 1. Electron energy-loss spectrum of amorphous boron nitride on carbon (sample courtesy of Dr K. Tanaka, Japanese National Institute for Research in Inorganic Materials). From left to right: the zero-loss peak, valence-loss peak, a detector-gain increment (× 400) and K-shell ionization edges of boron, carbon, nitrogen and (less prominently) oxygen. Because the inelastic scattering probability decreases rapidly with energy loss E, the electron intensity is conveniently represented on a logarithmic vertical scale.

Elastic scattering is responsible for most of the contrast in the images produced by a transmission electron microscope and also for most of the angular spreading of a beam within a specimen (figure 2). For 100 keV incident electrons, a typical scattering angle is 20 mrad (*ca.* 1°) per elastic collision.

If the specimen is crystalline, the regularity of the atomic spacing permits only certain preferred angles of scattering. The resulting diffraction pattern can be observed and photographed by using the electron microscope, and subsequent analysis of the pattern may enable the crystal structure and lattice parameters to be determined, which in turn may indicate the presence of a particular chemical compound. However, one limitation of this diffraction method of analytical electron microscopy is that many samples, including most biological ones, are practically amorphous and do not produce distinctive diffraction patterns.

PHILOSOPHICAL TRANSACTIONS OF THE ROYAL SOCIETY A MATHEMATICAL, PHYSICAL & ENGINEERING SCIENCES
PHILOSOPHICAL TRANSACTIONS OF THE ROYAL SOCIETY A MATHEMATICAL, PHYSICAL & ENGINEERING SCIENCES

Downloaded from rsta.royalsocietypublishing.org

MATHEMATICAL, PHYSICAL & ENGINEERING SCIENCES
PHILOSOPHICAL TRANSACTIONS OF THE ROYAL SOCIETY A

(b) *Inelastic scattering*

In passing through the sample, an accelerated electron can also interact directly with one or more atomic electrons. Since the latter have a mass comparable with that of the incident electron, appreciable energy transfer can occur. If the scattering takes place from *valence* electrons, this energy transfer is typically 10–100 eV. Valence-electron scattering is observed in the energy-loss spectrum in the form of one or more peaks in the 10–40 eV range (see figure 1). The scattering probability is comparable with that for elastic scattering, but scattering angles are less (typically *ca.* 2 mrad).

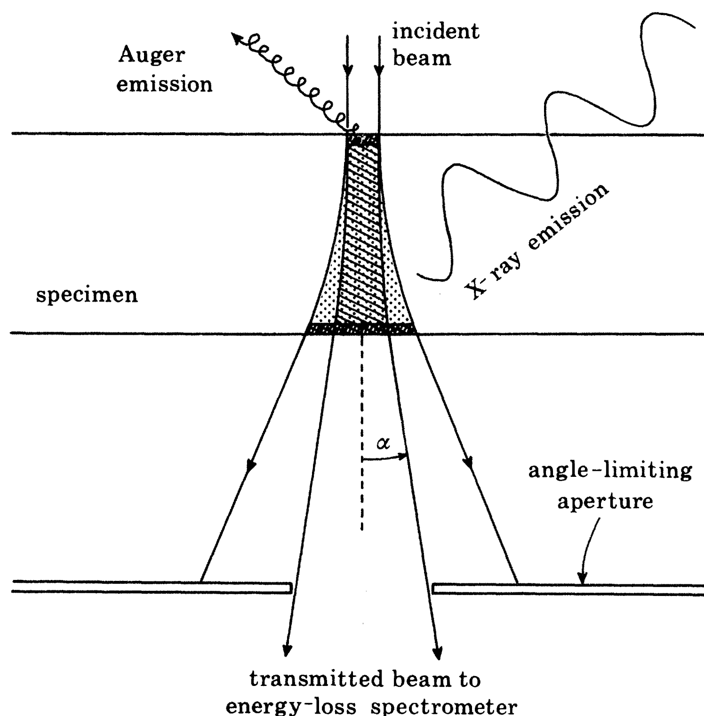

FIGURE 2. Transmission of an electron beam through a thin sample, showing the regions within the specimen that give rise to emitted X-rays (dotted), to the energy-loss signal (inner cone, shown hatched) and to Auger electrons (cross-hatched regions adjacent to both surfaces). The angular spreading of the beam is due mainly to elastic scattering.

Alternatively, an incident electron may be scattered by an *inner-shell* atomic electron. The latter is able to make a transition to a vacant energy level only if the energy transferred exceeds the ionization energy of that particular shell. Such events are observable in the energy-loss spectrum as an abrupt rise in intensity at an energy loss equal to each inner-shell ionization energy (see figure 1). These are referred to as ionization edges, and are the electron-beam analogue of absorption edges that occur in an X-ray absorption spectrum.

Ionization energies depend on the type of shell (K, L, etc.) and on the atomic number of the atom involved. Their values have been accurately determined for all the elements and are not greatly affected by the chemical environment of an atom. Therefore, detection of ionization edges in an energy-loss spectrum enables elements present within the specimen to be identified.

MATHEMATICAL, PHYSICAL & ENGINEERING SCIENCES
PHILOSOPHICAL TRANSACTIONS OF THE ROYAL SOCIETY A

Downloaded from rsta.royalsocietypublishing.org

It is the secondary processes, after inner-shell ionization, that give rise to the generation of X-rays and Auger electrons. When a vacant electron state in an inner shell is filled by a nearby valence electron, an amount of energy equal to the inner-shell ionization energy is released and carried away by an X-ray photon, or else given to an electron from another shell, which may then escape as an Auger electron. In either case, the photon or electron energy is characteristic of the emitting atom and therefore carries chemical information. However, the Auger electrons (which have comparatively low kinetic energy) are strongly scattered inside a solid and tend to be absorbed unless generated within a few monolayers of the surface. Auger spectroscopy therefore detects only elements that lie very close to the surface of a specimen (see figure 2). Although this surface sensitivity is very useful for some purposes, the technique will not be dealt with here; the reader is referred to the article by Rivière (this symposium).

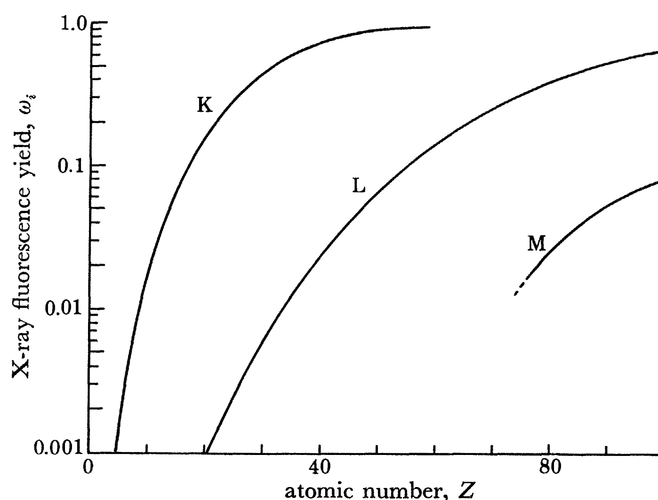

FIGURE 3. X-ray fluorescence yield, ω_i, for K, L and M shells, as a function of the atomic number, Z, of the emitting atom; ω_i represents the fraction of inner-shell ionizations that result in X-ray emission, and is therefore equal to the ratio of the number of X-ray photons to the number of energy-loss electrons produced by the ionization of a given shell.

X-ray photons are less strongly absorbed and can provide chemical information from anywhere within a specimen that is thin enough to transmit the incident beam (figure 2). But the X-ray fluorescence yield falls with decreasing atomic number of the emitting atom, Auger emission being the preferred mechanism of energy release in the lighter elements (see figure 3). Mainly for this reason, X-ray emission spectroscopy is relatively insensitive to elements lighter than sodium.

However, the low X-ray yield does not affect the energy-loss signal, since the latter arises directly from the *primary* ionization process. Eels therefore provides a useful complement to X-ray spectroscopy, particularly for analysis of elements near the beginning of the periodic table. It is quite feasible to combine both techniques in a single instrument, for example by having an X-ray spectrometer attached to the side of the electron microscope column (as close as possible to the specimen) and an electron spectrometer mounted underneath (below the viewing screen and plate camera).

By using an aperture to restrict the angular range of scattering allowed into the electron spectrometer, the region of specimen contributing to the energy-loss spectrum can be controlled

MATHEMATICAL, PHYSICAL & ENGINEERING SCIENCES
THE ROYAL SOCIETY A
PHILOSOPHICAL TRANSACTIONS OF
MATHEMATICAL, PHYSICAL & ENGINEERING SCIENCES
THE ROYAL SOCIETY A
PHILOSOPHICAL TRANSACTIONS OF

Downloaded from rsta.royalsocietypublishing.org

(see figure 2). In contrast, the entire irradiated volume contributes to the X-ray spectrum, this volume being larger because of the angular spreading of the transmitted beam (see figure 2). This means that the Eels method is capable of greater (lateral) spatial resolution; in fact, elements such as phosphorus have been detected with an estimated resolution better than 1 nm (Ottensmeyer & Andrew 1980).

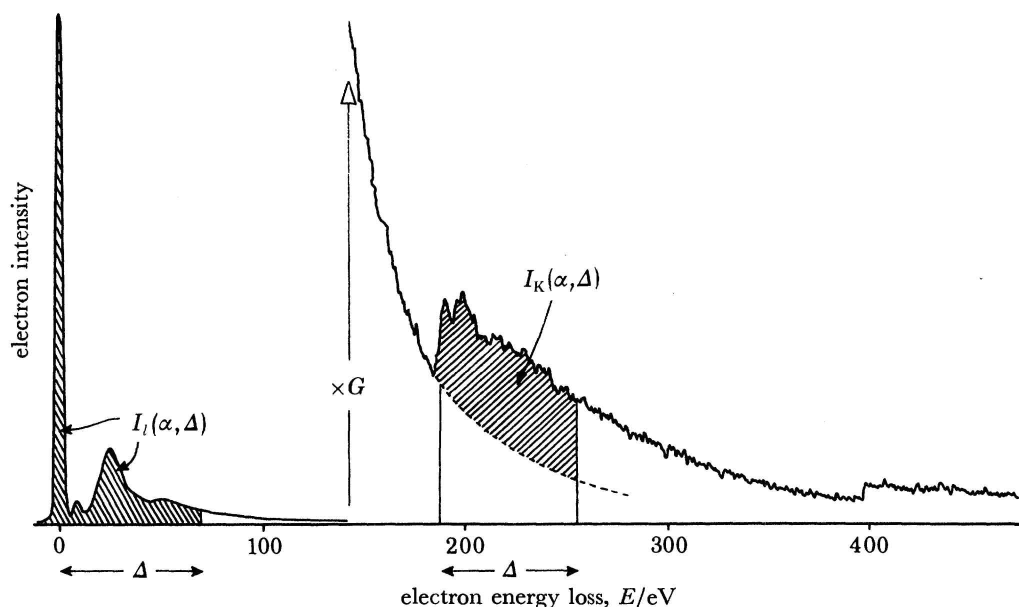

FIGURE 4. Energy-loss spectrum of crystalline boron nitride, showing the boron K-edge (at 190 eV) and the nitrogen K-edge (at 400 eV). The dashed curve is the background intensity (due here to inelastic scattering by valence electrons) extrapolated beneath the boron K-edge. The hatched areas represent the measured values required for the quantitative analysis of boron. In this example, the integration range is $\Delta = 70$ eV and the acceptance semi-angle of the spectrometer was $\alpha = 8.4$ mrad.

3. Quantitative analysis by energy-loss spectroscopy

Whereas quantitative results from X-ray spectroscopy are usually obtained as elemental ratios and by comparison with a standard sample of known composition, Eels is capable of giving absolute (standardless) quantitation. The concentration, N, of a measured element, in atoms per unit *area* of the specimen, is given by

$$N \approx \frac{1}{G\sigma_i(\alpha, \Delta)} \left[\frac{I_i(\alpha, \Delta)}{I_l(\alpha, \Delta)}\right]. \tag{1}$$

In this equation, α is the maximum angle of scattering allowed into the spectrometer, Δ is an energy range of integration within the energy-loss spectrum (see figure 4), G is a factor that takes into account any difference in detector gain between the low-energy and high-energy regions of the spectrum, and $\sigma_i(\alpha, \Delta)$ is an ionization partial cross section, which can be calculated (Egerton 1979*a*; Leapman *et al.* 1980). The quantity $I_l(\alpha, \Delta)$ is obtained by integrating the energy-loss intensity over a range Δ, starting at the zero-loss peak (see figure 4). The inner-shell intensity $I_i(\alpha, \Delta)$ (where i indicates the type of shell: K, L, etc.) is obtained by integration under the appropriate ionization edge, making due allowance for the background intensity (figure 4). Fortunately, the latter often displays a power-law dependence on energy loss:

PHILOSOPHICAL TRANSACTIONS OF THE ROYAL SOCIETY A MATHEMATICAL, PHYSICAL & ENGINEERING SCIENCES

PHILOSOPHICAL TRANSACTIONS OF THE ROYAL SOCIETY A MATHEMATICAL, PHYSICAL & ENGINEERING SCIENCES

Downloaded from rsta.royalsocietypublishing.org

$A\,E^{-r}$, where A and r can be assumed constant over a limited range of energy loss E. By sampling the background just preceding the ionization edge, the values of A and r can be determined. This type of data processing may be done rapidly if the spectrum is stored electronically in a multichannel analyser that is capable of being programmed to do simple arithmetic operations (Joy & Maher 1981).

Equation (1) can be rewritten in terms of the concentration *ratio* of two elements, in which case $I_l(\alpha, \Delta)$ cancels (and need not be measured) if the same integration range Δ is used for each ionization edge. The equation has been found to be sufficiently accurate provided that the thickness of the analysed region of the specimen is less than the mean free path for valence-electron inelastic scattering, which is typically about 100 nm for 100 keV incident electrons. In fact, such thin specimens are required anyway, to avoid an excessively high background level in the energy-loss spectrum, due to multiple valence-electron scattering. This illustrates one limitation of Eels elemental analysis: the analysed region of the specimen should be somewhat thinner than normally required for transmission electron microscopy or X-ray emission analysis. For some materials, this places unrealistic demands on the specimen preparation; in that situation, a possible solution may be to use a *high-voltage* microscope fitted with an energy-loss spectrometer, since for 1 MeV incident electrons the valence-electron mean free path is increased by about fourfold (Jouffrey *et al.* 1978).

Even with suitably thin specimens, the ratio of background to characteristic signal is usually higher in energy-loss spectra than in X-ray emission spectra. Therefore Eels is not as good at detecting elements whose concentration is small (less than 1%) relative to the other constituents of a sample.

4. Some applications

(*a*) *Analysis of thin films*

One type of application that exploits the absolute quantitation possible by Eels is the measurement of oxide thickness on a metal. If the latter can be dissolved away or made sufficiently thin, measurement of the oxygen K-ionization edge leads to an estimate of the oxide thickness. In this way, the oxide thickness on samples of aluminium, beryllium and magnesium was found to be 3, 5 and 20 nm, respectively (Egerton 1979*b*).

Thin films of dielectrics are used in the electronics industry for fabricating capacitors and switching devices. Their electrical characteristics depend on the chemical composition of the film, which might best be measured by Eels because light elements are often involved. Figure 1 shows an energy-loss spectrum of amorphous boron nitride deposited onto a thin carbon support film by reactive sputtering in the presence of oxygen. In addition to the zero-loss and valence-electron peaks, K-shell ionization edges due to boron, carbon, nitrogen and (less visibly) oxygen are observed. Measurements on these edges indicated a boron:nitrogen ratio close to unity and an oxygen content of about 10% in the film. In a similar way, the oxygen concentration in silicon oxide dielectric can be measured by Eels (Egerton 1979*b*).

(*b*) *Layer compounds*

Some solids (such as graphite and transition metal dichacogenides) have weak bonding in one crystallographic direction, allowing them to be easily cleaved into specimens thin enough for transmission electron microscopy and spectroscopy. Moreover, various chemical species (frequently containing light elements) can be incorporated between the atomic layers, giving

MATHEMATICAL, PHYSICAL & ENGINEERING SCIENCES
THE ROYAL SOCIETY A
PHILOSOPHICAL TRANSACTIONS OF

MATHEMATICAL, PHYSICAL & ENGINEERING SCIENCES
THE ROYAL SOCIETY A
PHILOSOPHICAL TRANSACTIONS OF

Downloaded from rsta.royalsocietypublishing.org

rise to a variety of intercalation compounds, some of which are currently of commercial interest (Thomas *et al.* 1981). The composition of such compounds is often variable and Eels may offer a method for measuring composition and local variations in composition with a spatial resolution determined mainly by the diameter of the incident electron beam. The composition of samples of graphite bisulphate and graphite oxide has been measured by this means, although care must be taken to keep the incident beam current sufficiently low to prevent radiolytic dissociation in the electron beam (Egerton 1979*b*).

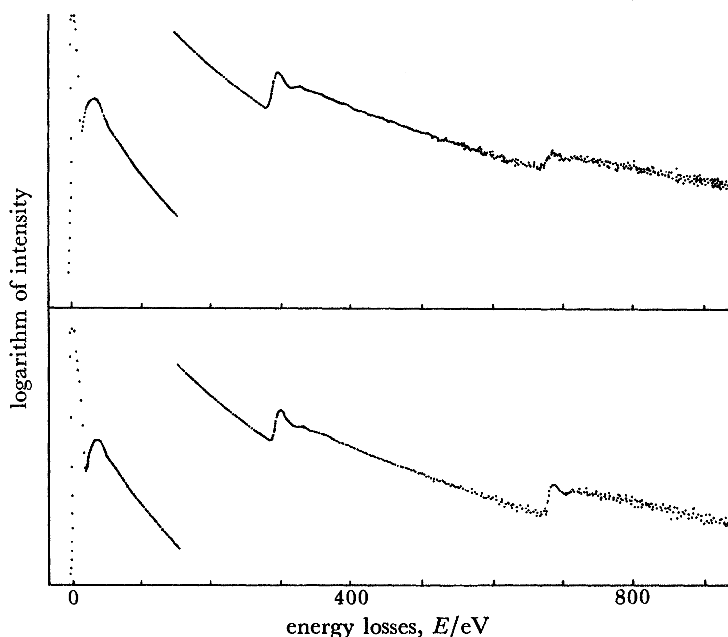

FIGURE 5. Electron energy-loss spectra of graphite fluoride, showing carbon and fluorine K-edges from which the fluorine:carbon ratio was measured to be 0.47 (upper spectrum) and 0.94 (lower spectrum). The samples were supplied by Dr N. Watanabe, Kyoto University.

Although not strictly an intercalation compound, graphite fluoride retains the property of easy cleavage and is used as a high-temperature lubricant, and also for the electrodes of a lithium battery (Watanabe 1980). Energy-loss spectra of two types of graphite fluoride are shown in figure 5. From measurements on the carbon and fluorine K-edges, the fluorine:carbon ratio was estimated to be 0.47 and 0.94 for the two samples.

Besides giving chemical information, Eels is capable of yielding structural information on an atomic scale. For example, fine structure in the energy-loss spectrum close to an ionization edge reflects the energy dependence of the density of electronic states above the Fermi level (Egerton & Whelan 1974). In the case of a ferric chloride – graphite intercalate, the additional electron states due to the intercalant species ($FeCl_3$) show up as an increase in the spectral intensity just ahead of the K-ionization edge of carbon (see figure 6). Intercalation also introduces a small chemical shift in the carbon K-level, visible in figure 6 as a slight displacement in the ionization edge. The *low-energy* region of the loss spectrum (up to 40 eV) can also be used to characterize the intercalant states, for example in potassium-intercalated graphite (Hwang *et al.* 1980; Ritsko 1981).

Downloaded from rsta.royalsocietypublishing.org

In addition, modulations in the electron intensity, extending over 100 eV or more on the high-energy side of an ionization edge, can be used to provide *structural* information concerning the *local* atomic environment of the corresponding element (Colliex *et al.* 1976). This is the electron-beam equivalent of Exafs modulations in an X-ray absorption spectrum, with the advantage that the incident electron beam can be focused onto very small specimen areas. Batson & Craven (1979) have demonstrated that it is possible to distinguish between different forms of carbon by using an incident beam only 1 nm in diameter.

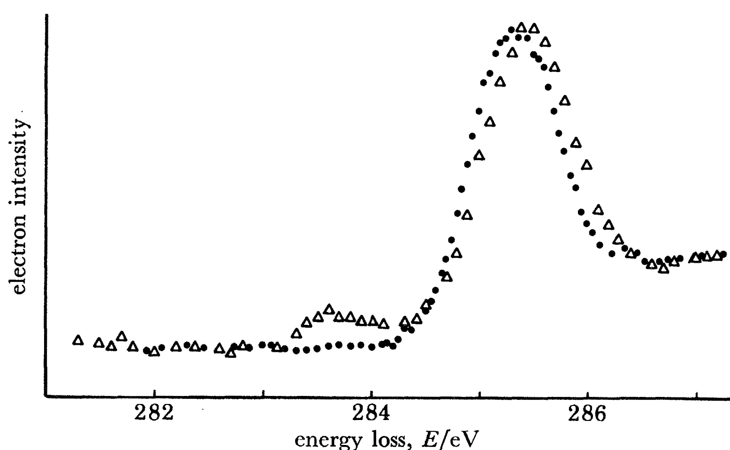

FIGURE 6. K-ionization edge of carbon recorded from graphite (●) and from stage 1 $FeCl_3$-intercalated graphite (△), by using a high-resolution spectrometer (Ritsko 1981).

(*c*) *Minerals, ceramics and metallurgical specimens*

Eels provides a suitable method of analysing coal specimens because although sulphur and metallic elements can be readily detected by X-ray emission spectroscopy, the nitrogen and oxygen content cannot be measured with comparable sensitivity by that method. Figure 7*a* shows the energy-loss spectrum from a sample of Pittsburgh Seam coal. K-ionization edges of nitrogen and oxygen are only faintly visible above the background provided by the carbon K-edge. But after subtracting this background (figure 7*b*), the nitrogen and oxygen edges are clearly visible, even in the presence of statistical noise associated with the measurement. The analysis of a typical area gave a nitrogen:carbon atomic ratio of 0.015 and an oxygen:carbon ratio of 0.06. Several laboratories are currently developing parallel-detection systems for Eels, which should markedly improve the signal:noise ratios in the energy-loss spectrum and make it easier to measure small atomic concentrations.

Eels has been used by Herrmann *et al.* (1980) to determine the local composition of a Si–Al–O–N ceramic that also contained magnesium. Figure 8 shows their energy-loss spectra from a crystalline grain (solid curve) and from amorphous material present at grain boundaries and triple points (dotted curve). A comparison of the two spectra indicates that Mg, Si and O are present with greater concentration at the grain boundaries, probably in the form of amorphous magnesium silicate. This type of information is of value in understanding the sintering process in multicomponent ceramics.

Bourdillon *et al.* (1981) have used Eels and X-ray emission spectroscopy to characterize samples of hot-pressed silicon carbide ceramic containing 1% boron and 1% carbon additives. Such materials are being investigated as replacements for high-temperature metal alloys in

PHILOSOPHICAL TRANSACTIONS OF THE ROYAL SOCIETY A MATHEMATICAL, PHYSICAL & ENGINEERING SCIENCES

PHILOSOPHICAL TRANSACTIONS OF THE ROYAL SOCIETY A MATHEMATICAL, PHYSICAL & ENGINEERING SCIENCES

Downloaded from rsta.royalsocietypublishing.org

gas-turbine engines and for bearings and seals. Only carbon could be detected at grain boundaries; the boron was found segregated in second-phase particles, in combination with carbon, vanadium, oxygen, chromium and iron.

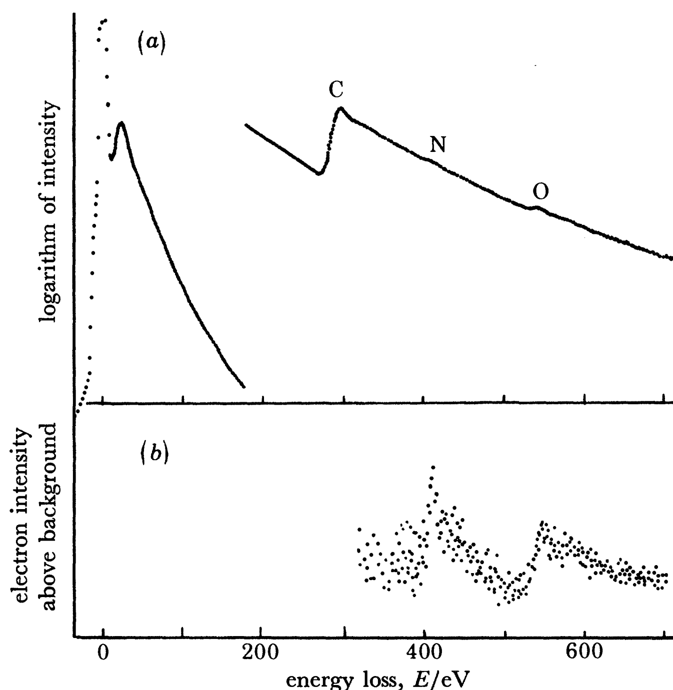

FIGURE 7. (*a*) Energy-loss spectrum of Pittsburgh Seam coal, showing carbon, nitrogen and oxygen K-ionization edges (specimen courtesy of S. Mehta, Bethlehem Steel Corporation). The spectrum was recorded serially, the total scan time being 1 min. (*b*) The nitrogen and oxygen K-edges, after subtracting the background intensity due to carbon K-shell ionization.

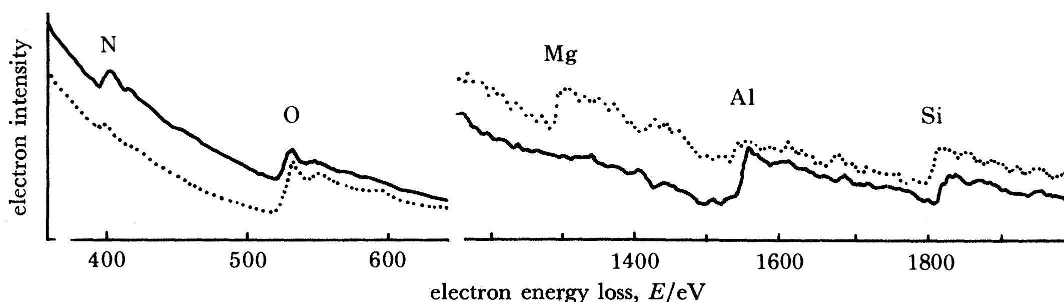

FIGURE 8. Energy-loss spectra of a Si–Al–O–N–Mg ceramic (Herrmann *et al.* 1980). The solid line represents data recorded from the interior of a grain, whereas the dots represent measurements from a triple-point region.

Another area of considerable commercial interest is the identification of carbide and nitride precipitates in various types of steel. Zaluzec (1980) used Eels to identify 200 nm diameter TiC and TiN precipitates; although crystalline, these both have the same crystal structure and very similar lattice parameters, so cannot readily be distinguished by electron diffraction. Also using the energy-loss spectrum, Leapman *et al.* (1978) identified the composition of needle-shaped precipitates in Cr–Mo steel as Cr_2N and that of granular precipitates as $Fe_5Cr_{18}C_6$.

PHILOSOPHICAL TRANSACTIONS OF THE ROYAL SOCIETY A MATHEMATICAL, PHYSICAL & ENGINEERING SCIENCES

PHILOSOPHICAL TRANSACTIONS OF THE ROYAL SOCIETY A MATHEMATICAL, PHYSICAL & ENGINEERING SCIENCES

Downloaded from rsta.royalsocietypublishing.org

Jouffrey & Sevely (1976) have used their 1 MeV microscope (fitted with an electron spectrometer) to characterize grains of lunar rock that were too thick (*ca.* 1 μm) to transmit electrons of lower energy. They found no evidence for a concentration of titanium at the surface of the grains, as had earlier been postulated.

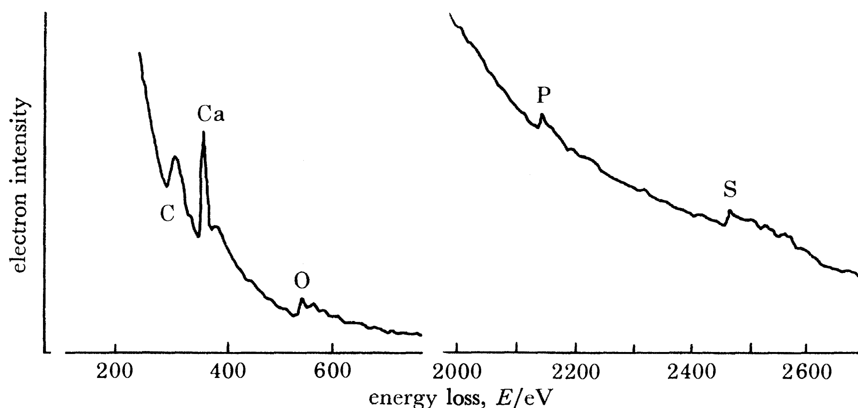

FIGURE 9. Part of the energy-loss spectrum from a thin section of a cultured osteoblast from rat tibia (Ottensmeyer & Andrew 1980).

(*d*) *Biological specimens*

Besides carbon, nitrogen and oxygen, biological tissue may contain elements such as sodium, calcium, phosphorus and sulphur. It is sometimes important to analyse for these elements with as high a spatial resolution as possible, to answer questions related to intracellular and intercellular transport.

Figure 9 shows the energy-loss spectrum from an extracellular deposit within a thin section of cartilage tissue. The presence of calcium is visible (in the form of a sharply-peaked L-edge) and also carbon, oxygen, phosphorus and sulphur (via their K-edges). By means of *energy-filtered imaging*, in which only those electrons occurring within a desired range of the energy-loss spectrum are selected by the spectrometer to form an image, the spatial distribution of a particular element can be mapped in two dimensions. The spatial resolution within an image formed from the phosphorus L-shell loss was estimated to be better than 1 nm, which corresponds to a detection of less than 10^{-20} g of phosphorus (Ottensmeyer & Andrew 1980; Bazett-Jones & Ottensmeyer 1980).

It may be possible to trace the uptake and localization of a particular organic compound within certain types of cell by using the analogous fluorine-substituted compound and detecting the fluorine distribution by Eels. Using fluorine K-loss electrons, Costa *et al.* (1978) have obtained energy-filtered images of human blood platelets to show that serotonin (or, at least, its fluorinated derivative) becomes concentrated in dense bodies within the cell.

Eels has also been used to detect the presence of metals in biological samples, for example beryllium grains in lung tissue (Jouffrey *et al.* 1978) and titanium within tumour cells treated with a titanium-containing antitumour agent (Köpf-Maier & Krahl 1981).

(*e*) *Measurement of radiation damage*

One difficulty associated with any electron-beam method of microanalysis, when applied to organic or biological specimens, is the removal of light elements (particularly gaseous ones) due

Downloaded from rsta.royalsocietypublishing.org

MATHEMATICAL, PHYSICAL & ENGINEERING SCIENCES
THE ROYAL SOCIETY A
PHILOSOPHICAL TRANSACTIONS OF

to the irreversible breakage of chemical bonds caused by the incident electrons. Since Eels is the most sensitive technique for analysing very light elements, it provides an ideal means of studying this 'mass loss' process and its dependence on experimentally controllable parameters. For various synthetic and biological polymers, it has been found that the loss of carbon, nitrogen and oxygen decays exponentially with electron dose, is independent of dose rate and specimen thickness (within the range normally encountered in biological electron microscopy) and is drastically reduced by cooling the sample during exposure to the electron beam (Egerton 1981). The disruption of chemical bonds can also be observed from the loss of fine structure within the electron energy-loss spectrum, both in the vicinity of ionization edges and within the 0–40 eV region (Isaacson *et al.* 1973).

These studies of electron-irradiation damage are directly related to high-resolution electron microscopy of biological specimens (where the extent of the damage largely determines the ultimate spatial resolution obtainable). They are also relevant to recent methods of fabricating very compact microelectronic circuits, where the 'damaging' effect of the electron beam is purposely used to polymerize an organic layer to make it susceptible to chemical attack.

References (Egerton)

Batson, P. & Craven, A. 1979 *Phys. Rev. Lett.* **42**, 893–897.
Bazett-Jones, D. P. & Ottensmeyer, F. P. 1980 *Science, Wash.* **211**, 169–170.
Bourdillon, A. J., Jepps, N. W., Stobbs, W. M. & Krivanek, O. L. 1981 *J. Microsc.* **124**, 49–56.
Colliex, C., Cosslett, V. E., Leapman, R. D. & Trebbia, P. 1976 *Ultramicroscopy* **1**, 301–315.
Costa, J. L., Joy, D. C., Maher, D. M., Kirk, K. & Hui, S. W. 1978 *Science, Wash.* **200**, 537–539.
Egerton, R. F. 1979*a* *Ultramicroscopy* **4**, 169–179.
Egerton, R. F. 1979*b* In *37th Annual Proc. Electron Microscopy Soc. Am.* (ed. G. W. Bailey), pp. 128–129. Baton Rouge: Claitor's Publishing Division.
Egerton, R. F. 1980 *Ultramicroscopy* **5**, 521–523.
Egerton, R. F. & Whelan, M. J. 1974 *J. Elect. Spectrosc. rel. Phenomena* **3**, 232–236.
Hermann, K.-H., Krahl, D., Rühle, M. & Kirn, M. 1980 In *Electron microscopy 1980* (ed. P. Brederoo & V. E. Cosslett), vol. 3, pp. 68–69. Leiden: 7th European Congress on Electron Microscopy Foundation.
Hwang, D. M., Utlaut, M., Isaacson, M. S. & Solin, S. A. 1980 *Physica* B **99**, 435–440
Jouffrey, B., Kihn, Y., Perez, J. P., Sevely, J. & Zanchi, G. 1978 In *Electron microscopy 1978* (ed. J. M. Sturgess), pp. 292–303. Toronto: Microscopical Society of Canada.
Jouffrey, B. & Sevely, J. 1976 *Revue Phys. Appl.* **11**, 101–111.
Hillier, J. & Baker, R. F. 1944 *J. appl. Phys.* **15**, 663–676
Isaacson, M. S., Johnson, D. & Crewe, A. V. 1973 *Radiat. Res.* **55**, 205–224.
Joy, D. C. & Maher, D. M. 1981 *J. Microsc.* **124**, 37–48
Köpf-Maier, P. & Krahl, D. 1981 *Naturwissenschaften* **68**, 273–274.
Leapman, R. D., Sanderson, S. J. & Whelan, M. J. 1978 *Metal Sci.*, April, 215–220.
Leapman, R. D., Rez, P. & Mayers, D. F. 1980 *J. chem. Phys.* **72**, 1232–1243.
Ottensmeyer, F. P. & Andrew, J. W. 1980 *J. Ultrastruct. Res.* **72**, 336–348.
Ritsko, J. J. 1980 In *39th Annual Proc. Electron Microscopy Soc. Am.*, pp. 174–177. Baton Rouge: Claitor's Publishing Division.
Thomas, J. M., Millward, G. R. & Bursill, L. A. 1981 *Phil. Trans. R. Soc. Lond.* A **300**, 43–49.
Watanabe, N. 1980 *Solid State Ionics* **1**, 87–110.
Zaluzec, N. J. 1980 *38th Annual Proc. Electron Microscopy Soc. Am.* (ed. G. W. Bailey), pp. 98–101. Baton Rouge: Claitor's Publishing Division.

Discussion

A. F. Fell (*Heriot-Watt University, Edinburgh, U.K.*). Recently Pavlath & Millard examined the application of various data processing algorithms in X-ray photoelectron spectroscopy (*Appl. Spectrosc.* **33**, 502–509 (1979)). In particular they demonstrated that, by transforming spectral profiles not dissimilar to those that Professor Egerton has shown for electron energy-loss

Downloaded from rsta.royalsocietypublishing.org

spectra to the second or fourth derivative (with respect to energy), resolution of adjacent features was improved and minor features were more easily detected. Has Professor Egerton considered applying this approach in his own work?

R. F. EGERTON. Several experimentalists have tried recording first-derivative energy-loss spectra, using a modulation technique akin to that employed (for example) in Auger spectroscopy. The results were not too encouraging, probably because of the relatively large statistical noise component at high energy loss, which is accentuated by differentiation.

A. F. FELL. One of Professor Egerton's spectra was particularly interesting in the context of the higher derivative technique. The principal peak was superimposed upon a curved baseline, which he examined at lower energy just before the peak in order to fit a polynomial function which, when extrapolated under the peak, would permit more accurate measurement of the peak area for quantitative purposes. In our experience, based largely on u.v.–visible and fluorescence spectroscopy, systematic interference of this nature is readily reduced, if not eliminated, by transforming the spectrum to an appropriate derivative. In general, if the observed baseline can be fitted by a polynominal of degree n, then the derivative or order $(n+1)$ should reduce the baseline contribution to negligible proportions. Moreover, the analytical peak of interest can be readily quantitated in the derivative spectrum, simply by measuring its amplitude in a standardized manner. An alternative approach to quantitation, little tried in practice, is to measure the area of the derivative peak within defined energy limits. In several cases of severe matrix interference, comparable with the example that Professor Egerton presented, we have found that an analysis based on the even derivative spectrum yields accurate data free of error due to variable matrix background. However, it should be noted that precision may be reduced in consequence of the increased noise level commonly observed in currently available derivative devices, although in some cases, where the variability of the background is inherently high, precision has been actually improved, especially at the trace amount level (A. F. Fell, D. R. Jarvie & M. J. Stewart, *Clin. Chem.* **27**, 286–292 (1981)).

R. F. EGERTON. I thank Dr Fell for the reference and for his suggestions. In Eels, the curved background preceding an ionization edge is usually fitted to a power law rather than to a polynomial function of energy loss. Conceivably a polynomial fit might serve equally well, although a negative value of n would seem the most natural choice.

One consequence of taking derivatives of the energy-loss spectrum would be to amplify preferentially the fine structure present in an ionization edge, which depends not only on the type of atom being ionized but also on its atomic environment. Such amplification could be valuable in certain circumstances, for example to detect differences in coordination of a given atomic species in different compounds. But for the purposes of quantitative microanalysis, we need a measurement that reflects the concentration of a given element and which is as independent as possible of its environment. This is one reason why an area under the ionization edge is measured, rather than the height of the edge (the latter being equivalent to an area under the first-derivative spectrum), since edge height is more affected by the near-edge fine structure.

Likewise, high-frequency noise present in the recorded spectrum would be amplified with each successive derivative. The major noise component is shot noise, which can only be reduced by improving the collection efficiency (e.g. by using a parallel detection system) and by in-

Downloaded from rsta.royalsocietypublishing.org

creasing the incident beam current and recording time (within the limitations imposed by heating, contamination and radiation damage to the specimen).

Nevertheless, it seems likely that some form of data processing should be applicable to the energy-loss spectrum, in order to extract the characteristic signal from background and noise. Perhaps this might involve cross-correlation or signal recognition techniques, taking full advantage of the fact that both the approximate position and the approximate shape of the ionization edges are known for each element.

MATHEMATICAL, PHYSICAL & ENGINEERING SCIENCES
THE ROYAL SOCIETY A
PHILOSOPHICAL TRANSACTIONS OF

MATHEMATICAL, PHYSICAL & ENGINEERING SCIENCES
THE ROYAL SOCIETY A
PHILOSOPHICAL TRANSACTIONS OF